# Status Report

Andrew J Penner

November 5, 2008

## 1 Description of Project

In my thesis I will numerically solve the magnetohydrodynamic (MHD) equations for a fluid coupled to the Einstein equations in the Kerr spacetime. The astrophysical phenomenon that are thought to obey this type of setup are numerous. Such examples are active galactic nuclei, accretion disks, and supernova explosions. Since I am focusing on a stationary spacetime background I will be most interested in accretion phenomenon.

A particularly interesting example was studied back in the 1940's by Bondi-Hoyle-Lytton. They worked on a phenomenon commonly known as Bondi-Hoyle-Lyttleton accretion. This was originally a Newtonian phenomenon. The physical setup is simple, one immerses a massive body in some uniform medium. Now give the massive body some velocity. The idea is that the massive body is travelling through space at a constant velocity through a fluid. Conversely you may consider the fluid flowing past the body at the same speed, where the massive body is stationary. The relativistic analogue was investigated starting with Curtis Michel, with the spherical accretion problem in 1971. Spherical accretion situates a Schwarzschild black hole in a uniform medium and calculates the steady state solution. The dynamic case does not have much in the way of a closed form solution, and has been primarily treated by Font and Ibanez in a series of 4 papers moving from the Schwarzschild case through to Kerr. They conclude with the promise to investigate the full 3D case, however more literature searches turn up nothing yet.

This has been investigated for the hydrodynamic case, ($\vec{B} = 0$), however a literature search turns up nothing in the way of a the same accretion problem with a magnetic field embedded in the fluid. Furthermore, there has been some research done in the case where an accretion disk surrounds a Kerr hole in a torus, and this torus need not be perfectly orthogonal to the rotation axis of the black hole. Nothing appears to have been done in the simpler case where a rotating black hole is travelling through spacetime in a direction not orthogonal to the rotation axis.

An astrophysical application to this problem could come from the in-spiraling black hole. This is a hot topic for relativists, as there are numerous groups currently working on this problem, developing codes to track the event horizons, and overcome difficulties that arise from numerical issues such as numerical dissipation and maintenance of the no magnetic monopole constraint. However the initial data for these evolutions are still considered to be a weakly understood. Proper initial data will consider the two black holes coming from somewhere, and entering a coalescing orbit. However one is left asking, what about the material accumulated by these holes, and what about the formation of the circumbinary disks that inevitably form? Bondi-Hoyle-Lyttleton accretion is a simplified approximation to real accretion however it is a decent starting point.

For all instances I expect to evolve the system in terms of the 3 major stationary metrics, Minkowski, Schwarzschild, and fianlly Kerr. The first approximation I use is the thin disk approximation, which claims that all deviations from the polar angle $\theta = \Pi/2$ are negligible. Finally I will generalize to a full 3D evolution.

To begin I go over some of the fundamental properties of general relativity. For a full treatment please see one of a hundred books available on the topic.

## 2 Einstein Equations, and Conservation

The Einstein equations can be written as:

$$G_{\alpha\beta} = 8\pi T_{\alpha\beta} \tag{1}$$

where we adopt geometric units such that $G = c = 1$. Here $G_{\alpha\beta}$ is the Einstein tensor and $T_{\alpha\beta}$ is the stress energy tensor. This is a simple expression (at least in appearance) that relates the spacetime curvature ($G_{\alpha\beta}$ to the matter stress energy tensor $T_{\alpha\beta}$.

The evolution equations for the Einstein equations are derived from the divergence of the Einstein tensor. For a stationary metric we expect that

$$\nabla_\alpha G^{\alpha\beta} = 0 = \nabla_\alpha T^{\alpha\beta}$$

, with solutions long studied and understood, we can focus entirely on the right hand side.

For fluid systems there are fundamental conserved quantities that are required for the evolution of such a fluid. We have the conservation of stress energy;

$$\nabla_\alpha T^{\alpha\beta} = 0 \tag{2}$$

As well as the conservation of the baryon number;

$$\nabla_\alpha J^\alpha = 0 \tag{3}$$

where $J^\alpha = \rho_o u^\alpha$. Since we are further interested in the effects of an embedded magnetic field we need one more condition to be satisfied;

$$\nabla^*_\mu F^{\mu\nu} = 0 \tag{4}$$

where $F^{\mu\nu}$ is the Faraday tensor for electromagnetism.

These equations are highly nonlinear and require the use of a computer for their solution. Along the way, I will attempt to utilize as many symmetries as possible to attempt to reduce the computational load expected, as in reduced dimensionality, or viscosity. Ultimately I expect to be able to generalize these equations to the beginning stages of plasma evolutions where we have to consider more than just one type of particle as it evolves through time. However before diving into that future project I must study the MHD approximation, which will allow for a better understanding of the physics behind the plasma evolution. Furthermore I also expect to observe as many conserved quantities as possible such as the divergence of the magnetic field. From here I will list the work done on MHD, a lot of which came from the relativistic hydrodynamical work by Smarr, Hawley, Evans, Gammie, Olabarrieta, Rezzola and many more...[4, 5, 6, 8, 7, 9, 10]

# 3 Previous work

Numerical hydrodynamics dates back to the work done in spherical symmetry by May and White[2]. They developed dynamic coordinate analysis (The Lagrangian approach) using finite differencing. Artificial viscosity was introduced as a higher order phenomenon, so as to smooth out "shock" regions numerically without having a significant effect on the physical meaning of the data. They studied neutron star collapse and supernova explosions in spherical symmetry. Difficulties in generalization arise from the use of dynamic coordinates. To resolve this issue Wilson, produced what are now known as Eulerian coordinates, where the fluid moves in a fixed coordinate base. Now the equations could be solved using advective equations, however they still required the use of artificial viscosity to circumvent the shock regions, and allow the code to maintain stability. This approach is still used today, for the study of many astrophysical phenomenon, such as the merger of two neutron stars.

All of these methods are equally applicable to the magnetohydrodynamical equations. A fundamental property of the (magneto)hydrodynamic equations is that they may be all written in a conservative form. IE they may be generally written as:

$$\partial_t q + \partial_i f^i(q) = \Sigma(q) \tag{5}$$

where $q \to q(x_i, t)$ is a state vector of the fluid. $f^i$ is the flux vector, and $\Sigma$ is a source (also referred to as a production in some literature). The critical property of the source term is that it does not contain any

derivatives of the fluid variables. Any such terms must be written into the flux term. This gives us what is commonly referred to as a hyperbolic equations, which have a finite propagation velocity, as is expected in general relativity. This particular form allows us to use Godunov methods, also know as high resolution shock capturing methods. This approach will allow us to avoid the use of artificial viscosity, and consequently allow us to handle evolution which acquire more extreme shocks. In the case of extreme relativistic fluids, much larger $\gamma$ terms may be observed (ultra relativistic).

# 4 Hydrodynamic Equations

We start with the stress-energy conservation equation 2;

$$T^{\mu}_{\nu;\mu} = 0$$

we expand this into expressions involving a standard derivative and the Christoffel symbols

$$(T^{\mu}_{\nu})_{,\mu} + T^{\alpha}_{\nu}\Gamma^{\mu}_{\alpha\mu} - T^{\mu}_{\alpha}\Gamma^{\alpha}_{\mu\nu} = 0$$

There is a well know relation for a Christoffel symbol contracted over these two indices;

$$\Gamma^{\mu}_{\alpha\mu} = \frac{(\sqrt{-g})_{,\alpha}}{\sqrt{-g}} \tag{6}$$

so we are left with;

$$(T^{\mu}_{\nu})_{,\mu} + T^{\alpha}_{\nu}\frac{(\sqrt{-g})_{,\alpha}}{\sqrt{-g}} - T^{\mu}_{\alpha}\Gamma^{\alpha}_{\mu\nu} = 0$$

which after multiplying by the scalar $\sqrt{-g}$, reduces to;

$$(\sqrt{-g}T^{\mu}_{\nu})_{,\mu} = \sqrt{-g}T^{\mu}_{\alpha}\Gamma^{\alpha}_{\mu\nu}$$

where now to put it into a flux conservative form we expand the contraction in the left hand side into a time term and a space term

$$(\sqrt{-g}T^{t}_{\nu})_{,t} + (\sqrt{-g}T^{i}_{\nu})_{,i} = \sqrt{-g}T^{\mu}_{\alpha}\Gamma^{\alpha}_{\mu\nu} \tag{7}$$

so we see our conserved variables in these equations are going to involve the term $T^{t}_{\nu}$. We also note that there is an immediate occurrence of a source term if we look at any space other than Minkowski. This will be further broken down when I look at the actual form of the stress energy tensor for ideal MHD.

Next we look at the Baryon conservation equation 3;

$$J^{\mu}_{;\mu} = 0 \tag{8}$$

$$(\rho_o u^{\mu})_{;\mu} = 0$$

expanding returns

$$(\rho_o u^{\mu})_{,\mu} + (\rho_o u^{\alpha})\Gamma^{\mu}_{\alpha\mu} = 0$$

where we use equation 6 again;

$$(\rho_o u^{\mu})_{,\mu} + (\rho_o u^{\alpha})\frac{(\sqrt{-g})_{,\alpha}}{\sqrt{-g}} = 0$$

so ultimately we get;

$$(\sqrt{-g}\rho_o u^{t})_{,t} + (\sqrt{-g}\rho_o u^{i})_{,i} = 0$$

where we obtain another conservative variable $D = \rho_o u^t$.

Also for notational simplicity;

$$\begin{aligned} h &= 1 + \epsilon + \frac{P}{\rho_o} \\ \epsilon &= (\Gamma - 1)P/\rho_o \end{aligned} \tag{9}$$

Further, I will ignore hydrodynamic viscosity and thermal conductivity, to get the reader up to date on the field as it currently stands. I will relax this restriction later in the document.

To further specify the system we are also required to select an equation of state. $P \rightarrow P(\rho)$. For the relativistic gases I chose the ideal gas $P = (\Gamma - 1)\rho\epsilon$, however this will be altered later, when the zeroth order implementation of temperature is included.

# 5 Electromagnetic Equations

Finally we consider the Faraday condition 4

$$ {}^*F^{\mu\nu}_{;\nu} = 0 $$

which will break down exactly like that of the stress energy tensor

$$ ({}^*F^{\mu\nu})_{,\mu} + {}^*F^{\alpha\nu}\Gamma^{\mu}_{\alpha\mu} + {}^*F^{\mu\alpha}\Gamma^{\nu}_{\mu\alpha} = 0 $$

again using 6 so we are left with;

$$ ({}^*F^{\mu\nu})_{,\mu} + {}^*F^{\alpha\nu}\frac{(\sqrt{-g})_{,\alpha}}{\sqrt{-g}} + {}^*F^{\mu\alpha}\Gamma^{\nu}_{\mu\alpha} = 0 $$

which after multiplying by the scalar $\sqrt{-g}$, reduces to;

$$ (\sqrt{-g}\,{}^*F^{\mu\nu})_{,\mu} = \sqrt{-g}\,{}^*F^{\alpha\mu}\Gamma^{\nu}_{\mu\alpha} $$

where now to put it into a flux conservative form we expand the contraction in the left hand side into a time term and a space term

$$ (\sqrt{-g}\,{}^*F^{t\nu})_{,t} + (\sqrt{-g}\,{}^*F^{i\nu})_{,i} = \sqrt{-g}\,{}^*F^{\alpha\mu}\Gamma^{\nu}_{\mu\alpha} $$

This can be further broken down into 2 equations, when we consider the $\nu$ index alone, we separate space and time (t,j);

$$ (\sqrt{-g}\,{}^*F^{tt})_{,t} + (\sqrt{-g}\,{}^*F^{it})_{,i} = \sqrt{-g}\,{}^*F^{\alpha\mu}\Gamma^{t}_{\mu\alpha} $$
$$ (\sqrt{-g}\,{}^*F^{tj})_{,t} + (\sqrt{-g}\,{}^*F^{ij})_{,i} = \sqrt{-g}\,{}^*F^{\alpha\mu}\Gamma^{j}_{\mu\alpha} $$

Unlike the Stress-energy tensor, we know that the Faraday tensor is antisymmetric. The terms on the right hand side are now the fully contracted product of a symmetric and antisymmetric tensor. (The Christoffel symbols are symmetric in the lower indices.) Thus the right hand sides are identically zero. Furthermore the diagonal elements of $F^{\mu\nu}$ are also zero. Thus we are left with;

$$ (\sqrt{-g}\,{}^*F^{it})_{,i} = 0 $$
$$ (\sqrt{-g}\,{}^*F^{tj})_{,t} + (\sqrt{-g}\,{}^*F^{ij})_{,i} = 0 $$

We know from classical electrodynamics that the elements of the Faraday tensor of the form ${}^*F^{it}$ will be proportional to the magnetic field $B^i$ so the first expression looks like the no–magnetic–monopole condition. The second equation, is an evolution equation for the magnetic field.

To begin with I will assume ideal MHD, where the Electric field $E^{\mu}$ in the co-moving frame is zero, or $F_{\mu\nu}u^{\nu} = 0$ (the Lorentz force in the rest frame is zero). This an acceptable approximation since the observation in astrophysical phenomenon the magnetic Reynolds number is comparatively large, which then leads us to the assumption that the conductivity of the system tends to infinity. Further, one can use Ohm's law to write the electric current $J^{\mu}$ in terms of the magnetic field coupled to the fluid 4-velocity.

Mathematical implementation of this goes as follows; $\mathcal{J}^{\alpha} = \rho u^{\alpha} + \sigma F^{\alpha\nu}u_{\nu}$ must remain finite with $\sigma \rightarrow \infty$, so $F^{\mu\nu}u_{\nu} = 0 \rightarrow E_{\mu} = 0$ for a co-moving observer $u_{\alpha} = (1, 0, 0, 0)$. With this and the help of Jackson we have a transformation of the Faraday tensor between two frames of reference.

$$ \vec{E}' = \gamma\left(\vec{E} - \vec{v}\times\vec{B} - \frac{\gamma\left(\vec{v}\cdot\vec{E}\right)\vec{v}}{\gamma+1}\right) $$

So we get

$$\vec{E}' = \gamma(-\vec{v} \times \vec{B})$$

Thus allowing us to eliminate the electric field from the Faraday tensor, leaving us with a set of equations involving the magnetic field and the velocity field alone.

# 6 3+1 decomposition

Mostly you can refer to Matt's notes on this topic. What I need now;

$$\begin{bmatrix} g_{tt} & g_{jt} \\ g_{ti} & g_{ij} \end{bmatrix} = \begin{bmatrix} \beta_s\beta^s - \alpha^2 & \beta_j \\ \beta_i & \gamma_{ij} \end{bmatrix}$$

and

$$\begin{bmatrix} g^{tt} & g^{jt} \\ g^{ti} & g^{ij} \end{bmatrix} = \begin{bmatrix} -\frac{1}{\alpha^2} & \frac{\beta^j}{\alpha^2} \\ \frac{\beta^i}{\alpha^2} & \gamma^{ij} - \frac{\beta^i\beta^j}{\alpha^2} \end{bmatrix}$$

With this in mind we can define

$$W = \frac{1}{\sqrt{1 - g_{ij}v^iv^j}} = \frac{1}{\sqrt{1 - \gamma_{ij}v^iv^j}} \tag{10}$$

We define the normal vector;

$$n_\mu = (-\alpha, 0, 0, 0) \tag{11}$$

$$n^\mu = \left(\frac{1}{\alpha}, -\frac{\beta^i}{\alpha}\right) \tag{12}$$

With this in mind we define our velocity 4-vectors as;

$$v^i = \frac{u^i}{\alpha u^0} + \frac{\beta^i}{\alpha} = \frac{u^i}{W} + \frac{\beta^i}{\alpha} \tag{13}$$

$$u^0 = \frac{W}{\alpha} \tag{14}$$

$$v_j = \frac{u_j}{W} \tag{15}$$

We also define $\perp_{\mu\nu}$ to be

$$\perp_{\mu\nu} = g_{\mu\nu} + n_\mu n_\nu \tag{16}$$

We further define (as per Gammie & Noble Paper)

$$b^\mu = \frac{1}{W}h^\mu_\nu \mathcal{B}^\nu \tag{17}$$

$$h_{\mu\nu} = g_{\mu\nu} + u_\mu u_\nu \tag{18}$$

$$b_\mu = g_{\mu\nu}b^\nu \tag{19}$$

to be the 4-magnetic field variables.
$h_{\mu\nu}$ is the projection operator to take a vector into the space normal to the fluid 4-velocity $u^\mu$

# 7 Ideal MHD Stress Energy

We define the stress energy tensor for ideal MHD to be a linear combination of the stress energies for both the electromagnetic and hydrodynamic systems:

$$T^{EM}_{\mu\nu} = F_{\mu\sigma}F^{\sigma}_{\nu} - \frac{1}{4}g_{\mu\nu}F_{\alpha\beta}F^{\alpha\beta} = (\frac{1}{2}g_{\mu\nu} + u_\mu u_\nu)b^2 - b_\mu b_\nu \tag{20}$$

$$T^{Hydro}_{\mu\nu} = (\rho_o + \rho + P)u_\mu u_\nu + Pg_{\mu\nu} = \rho_o h u_\mu u_\nu + Pg_{\mu\nu} \tag{21}$$

$$T^{MHD}_{\mu\nu} = (\rho_o h + b^2)u_\mu u_\nu + (P + \frac{1}{2}b^2)g_{\mu\nu} - b_\mu b_\nu \tag{22}$$

where our definition of $b^\mu = \left(\frac{W}{\alpha}(\vec{v}\cdot\vec{\mathcal{B}}), \frac{\mathcal{B}^i}{W} + \alpha W(\vec{v}\cdot\vec{B})\left(v^i - \frac{\beta^i}{\alpha}\right)\right) = \left(\frac{W}{\alpha}(\vec{v}\cdot\vec{\mathcal{B}}), \frac{\mathcal{B}^i}{W} + \alpha b^0\left(v^i - \frac{\beta^i}{\alpha}\right)\right)$

# 8 Putting it all together

The final task for the EOM is to use the 3+1 formalism. This involves 3 transformations of the Stress-Energy tensor, and the magnetic field;

$$E = T^{\mu\nu}n_\mu n_\nu \tag{23}$$

$$S_i = T^{\mu\nu}n_\mu \perp_{\nu i} \tag{24}$$

$$\mathcal{B}^\mu = n^*_\nu F^{\mu\nu} \tag{25}$$

since $n_\mu = (-\alpha, 0, 0, 0)$;

$$E = T^{\mu\nu}n_\mu n_\nu = T^{tt}(-\alpha)^2 \tag{26}$$

$$= \alpha^2\left[(\rho_o h + b^2)(u^t)^2 - \left(P + \frac{1}{2}b^2\right)\frac{1}{\alpha^2} - (b^t)^2\right]$$

$$= (\rho_o h + b^2)W^2 - (P + \frac{1}{2}b^2) - (\alpha b^t)^2 \tag{27}$$

$$S_i = -T^{\mu\nu}n_\mu \perp_{\nu i} = \alpha T^{t\nu}\perp_{\nu i} = \alpha T^{t\nu}(g_{\nu i} + n_\nu n_i) \tag{28}$$

$$= \alpha T^t_i = \alpha(\rho_o h + b^2)u^t u_i - \alpha b^t b_i$$

$$= (\rho_o h + b^2)W^2 v_i - \alpha b^t b_i$$

$$\mathcal{B}^\mu = -n_\nu F^{\nu\mu} \tag{29}$$

$$\tag{30}$$

$$= \alpha F^{0\mu} \tag{31}$$

$$= \alpha B^\mu \tag{32}$$

I will further note that $n_\mu\mathcal{B}^\mu = 0$ so $\mathcal{B}^t = 0$.
From here we get the conserved quantities:

$$q = \begin{bmatrix} D \\ S_j \\ \tau \\ \mathcal{B}^k \end{bmatrix} \tag{33}$$

where $\tau = E - D$ which is used for the proper recovery of the Newtonian limit. We have the corresponding flux terms:

$$f(q) = \begin{bmatrix} D\hat{v}^i \\ S_j\hat{v}^i + P\delta^i_j - \frac{b_j B^i}{W} \\ \tau\hat{v}^i + Pv^i - \alpha\frac{b^t B^i}{W} \\ \mathcal{B}^k\hat{v}^i - \hat{v}^k\mathcal{B}^i \end{bmatrix} \tag{34}$$

where $\hat{v}^i = v^i - \frac{\beta^i}{\alpha}$

This leaves us with the generalized relativistic conservative form;

$$\frac{\partial}{\partial x^0}\sqrt{\gamma}\vec{q} + \frac{\partial}{\partial x^i}\sqrt{-g}\vec{f^i}(\vec{q}) = S(\vec{q}; x^\mu) \tag{35}$$

# 9 Characteristics and Finite Volume Methods

For hyperbolic equations such as the wave equation:

$$\frac{\partial^2\psi}{\partial t^2} = v^2\frac{\partial^2\psi}{\partial x^2}$$

or more simply the advection equation:

$$\frac{\partial\psi}{\partial t} = v\frac{\partial\psi}{\partial x}$$

there are two characteristic lines. These are the retarded and advanced coordinates $a = x+vt$, and $r = x-vt$. The final solution of this problem must be of the form $\psi = \alpha f(a) + \beta g(r)$, where the boundary conditions and initial conditions determine the correct forms of the functions $f, g$ as well as the coefficients $\alpha, \beta$. The importance of this fact is two fold, one all disturbances travel along the direction of the characteristics, the second is that these characteristics determine shock information about the system. Both of these pieces of information allow the user to determine the proper solution techniques for the problem.

Let's take a simple example:

$$a(x,t)u_t(x,t) + b(x,t)u_x(x,t) + c(x,t)u = 0$$

We want to switch from the coordinates $(x,t)$ to $(x_o, s)$ in which the PDE takes on the form of an ODE. Naturally we can then parameterize the original coordinates $(x(s), t(s))$. The new coordinate $x_o$ is constant along the characteristic curve, and is determined by the initial conditions on the coordinate system. With this we have:

$$\frac{du}{ds} = \frac{\partial x}{\partial s}u_x + \frac{\partial t}{\partial s}u_t$$

This is compared to our original PDE to get:

$$\frac{\partial t}{\partial s} = a(x,t)$$

and

$$\frac{\partial x}{\partial s} = b(x,t)$$

For our case we will have $a(x,t) = 1$ which simplifies matters slightly. From this piece of information we get: $t = s + t_o$, where $t_o$ is just an integration constant. Using that we solve our system from $t = 0$ and we get $t_o = 0$.

Now taking the second coefficient $b(x,t) = v$ where $v$ is a constant we can further solve the system to get $x(s)$:

$$\frac{\partial x}{\partial s} = v \rightarrow x = vs + x_o$$

We use again the initial condition on the coordinates $x(0) = x_o$ to solve for $x_o$ With our knowledge of $t = s$ we simplify matters but having a characteristic line equation

$$x = vt + x_o$$

where $x_o$ is the point on the x-axis of the x-t plane.

Expanding this idea into three dimensions is fairly straightforward.

The necessity of observing the characteristic lines comes from the need to understand the behaviour of the solution. For example, if shocks appear in the system, clearly a finite difference scheme fails, as derivatives across jumps are forbidden. Fortunately a method exists for just this case, the finite volume method. (Smoothed particle methods would also work however they do not capture shocks as well.) The finite volume method depends on an integral solution to the original PDE problem. This will be described later.

What makes this useful for us is that the Jacobian is not strictly constant, so the characteristic lines across a discontinuity may intersect. It is these intersections that indicate that the system may undergo shocks. A simple example of a shock comes from a system say a stationary fluid like air around an explosive device. When the device detonates we have an impulse of a high pressure high velocity region blowing out a relatively low pressure, low velocity region, compressing (shocking) the system.

Conversely if one sees that the characteristics diverge from each other across the discontinuity, then we have a rarefaction. An example of a rarefaction is a compressed spring released. Rarefaction waves expand with time, reducing pressure, and usually follow in the wake of a shock wave.

# 10 The method of Lines/Characteristics

Before moving on to discuss the finite volume method, I will take a quick foray into the method of lines (MOL). The MOL is a technique for treating PDE's as a system of ODEs. Typically this method discritizes an N-dimensional PDE's into one dimensional ODE's. These are applied to IBVP's only. Using this technique still requires that the spatial (typically) portion of the problem to be continuous across the entire domain. This is not always expected in fluid systems, and consequently is not the end of the line for our investigation.

Another useful technique is the method of characteristics. This method uses the characteristics defined in the last section for solving the PDE. For a hyperbolic system, since the disturbances propagate along the characteristics, we can treat the problem as an ODE along those characteristic lines. Consider:

$$\partial_t \vec{q} + \nabla_i F^i(\vec{q}) = \partial_t \vec{q} + \mathcal{J}(F)_i \partial_i \vec{q} = S(x_\mu; q)$$

where $\mathcal{J}$ denotes the Jacobian of the flux vector with respect to the variables $\vec{q}$. To determine the characteristic velocities and hence the characteristics for the system, we find the eigenvalues (characteristic speeds) and eigenvectors (characteristic directions) of the Jacobian matrix.

Now that we have the characteristic lines for the system at hand we are free to solve the ODE (using our old example PDE)

$$\frac{du}{ds} + c(x,t)u = 0$$

. which is valid along the characteristic lines.

The solution to this problem;

$$u(s) = exp \int c(x,t) ds$$

with $u(0) = f(x_o)$. For cases with no source terms we have that the solution is constant and is equal to the initial values.

The most restricting assumption on this method of solution is that the characteristic velocities are assumed constant for the particular time step. However for a time step which is sufficiently small this is a good approximation. It leads to methods defined below which closely approximate the Riemann problem but are much less computationally expensive.

One may look at the Burger's equation for some direction. The burger's equation is

$$u_t + u u_x = 0$$

so we have a variable coefficient on the spatial derivative term. Since the temporal coefficient is still unity, we expect the characteristic to be parameterized by time (t=s as seen earlier). This means that the solution

will not change with time along the characteristic (reword, not mine), so the system may still be treated as a total derivative:

$$\frac{du(x(t),t)}{dt} = u_x \frac{dx}{dt} + u_t = uu_x + u_t = 0$$

where we have matched

$$\frac{dx}{dt} = u(x,t)$$

Solving for the characteristic will involve knowledge of the initial condition on u $u(x_o, 0)$. The initial condition is constant, so the characteristics will be straight lines. (Of course may still intersect) The characteristic takes on the form $x = x_o + u(x_o, 0)t$, and the initial value problem will have the form:

$$u(x,t) = f(x_o) = f(x - ut)$$

and is clearly an implicit problem.

The significance of is that our system will behave very similar to the Burger's equation. We will have unity as a coefficient on the temporal derivative and a spatial derivative coefficient that depends on spacetime and the dynamic variables. So, although more complicated, it will have a similar form.

For a short time one may follow characteristics for a solution to the PDE. After long times, once the characteristics have intersected the solution is no longer single valued. This proves to be a problem since classical solutions to PDEs must be single valued, thus the concept of a weak solution was developed. Typically this involves integral solutions to the PDE, and consequently may have discontinuities. When one arrives at a 'weak solution, they must test the result to ensure that it is physical. This test comes in the form of the Rankine-Hugoniot jump condition.

Shock waves have a predictable velocity with comes about from the Rankine-Hugoniot condition. This condition governs the behaviour of shock waves normal to oncoming flow (reword). This equation considers a steady flow across a jump in initial data (time derivatives are zero) and demands a conservation of density, energy and momentum. Classically these are (for an ideal gas)

$$\rho_1 u_1 = \rho_2 u_2 \tag{36}$$

$$P_1 + \rho_1 u_1^2 = P_2 + \rho_2 u_2^2 \tag{37}$$

$$e_1 + \frac{P_1}{\rho_1} + \frac{1}{2}u_1^2 = e_2 + \frac{P_2}{\rho_2} + \frac{1}{2}u_2^2 \tag{38}$$

We have then rearrange the equations to keep the velocities on the left side.

$$\frac{u_1}{u_2} = \frac{\rho_2}{\rho_1} \tag{39}$$

$$\rho_1 u_1^2 - \rho_2 u_2^2 = P_2 - P_1 \tag{40}$$

$$u_1^2 - u_2^2 = 2(h_2 - h_1) \tag{41}$$

where $h = e + \frac{P}{\rho}$. Multiply the second equation by $\frac{1}{u_2^2}$ and using the first equation in the second:

$$\rho_1 \frac{u_1^2}{u_2^2} - \rho_2 = \frac{P_2 - P_1}{u_2^2} \rightarrow \rho_1 \frac{\rho_2^2}{\rho_1^2} - \rho_2 = \frac{P_2 - P_1}{u_2^2} \rightarrow \frac{\rho_2^2}{\rho_1} - \rho_2 = \frac{P_2 - P_1}{u_2^2}$$

Like wise for the third equation:

$$\frac{u_1^2}{u_2^2} - 1 = 2\frac{(h_2 - h_1)}{u_2^2} \rightarrow \frac{\rho_2^2}{\rho_1^2} - 1 = 2\frac{(h_2 - h_1)}{u_2^2}$$

Now solve for the velocity term $u_2^2$ in one equation and substitute in the other. After some algebraic manipulation we get:

$$2(h_2 - h_1) = (P_2 - P_1)(\frac{1}{\rho_1} + \frac{1}{\rho_2})$$

.

(That was fun, but it was Newtonian. There must be relativistic versions of the same thing.)

The other thing to consider is what is known as the Rankine-Hugoniot shock condition, again looking at the basic conservation law:

$$\int_{x_R}^{x_L}\int_{t_o}^{t} u_t dt dx + \int_{x_R,t_o}^{x_L,t} \partial_i F^i(u) dx dt = 0$$

$$\int\int_{x_R}^{x_L} u dx dt + \int (F^i(u(x_1)) - F^i(u(x_o)))dt = 0$$

looking at an infinitesimal time step, $s = \frac{dx}{dt}$, we have

$$u_L - u_R = s(F(u_L) - F(u_R))$$

so we have a demand on the shock speed for any conservation system:

$$s = \frac{F(u_L) - F(u_R)}{u_L - u_R}$$

This is the only allowable shock speed, any others are unphysical.

Since we no longer have a single valued solution (in the weak solution) we require the use of an entropy condition to pick out the physically correct solution. That condition is met through the Rankine-Hugonoit shock condition as described above.

# 11 The Solver

For this project I will be using the Finite Volume Method (FVM), which is a method to find weak integral solutions to hyperbolic PDEs. I describe The basics behind this method, for full details and a description of hyperbolic PDEs I refer you to LeVeque.

For a set of nonlinear conservation laws (5) we have:

$$\frac{1}{\sqrt{-g}}\frac{\partial\sqrt{\gamma}q}{\partial t} + \frac{1}{\sqrt{-g}}\frac{\partial\sqrt{-g}f^i(q)}{\partial x^i} = S(q)$$

We desire the integral form of this equation, so we integrate both parts over some small cell or volume in spacetime. The integral can be taken over a sufficiently small amount of spacetime, so that;

$$\int \frac{1}{\sqrt{-g}}\frac{\partial}{\partial t}\left(\sqrt{\gamma}q\right) dV^{(4)} + \int \frac{1}{\sqrt{-g}}\frac{\partial}{\partial x^i}\left(\sqrt{-g}f^i(q)\right) dV^{(4)} = \int S(q) dV^{(4)} \tag{42}$$

where $dV^{(4)} = \sqrt{-g}dx_0dx_1dx_2dx_3$.

Breaking up the integrals;

$$\int_{\Delta x_0}\int_{\Delta x^i} \frac{\partial}{\partial t}\left(\sqrt{\gamma}q\right) dx_1dx_2dx_3dx_0 + \int_{\Delta x_0}\int_{\Delta x^i} \frac{\partial}{\partial x^i}\left(\sqrt{-g}f^i(q)\right) dx_1dx_2dx_3dx_0 = \int_{\Delta x_0}\int_{\Delta x^i} S(q)\sqrt{-g}dx_1dx_2dx_3dx_0 \tag{43}$$

I define a cell average to be;

$$Q \approx \frac{1}{\Delta V^{(3)}}\int_{\Delta x^i}\sqrt{\gamma}q dx_1dx_2dx_3. \tag{44}$$

with $\Delta V^{(3)} = \sqrt{\gamma}\Delta x_1\Delta x_2\Delta x_3$.

So

$$\int_{\Delta x_0}\frac{\partial}{\partial t}Q\Delta V^{(3)}dx_0 + \int_{\Delta x_0}\int_{\Delta x^i}\frac{\partial}{\partial x^i}\left(\sqrt{-g}f^i(q)\right)dx_1dx_2dx_3dx_0 = \int_{\Delta x_0}\int_{\Delta x^i} S(q)\sqrt{-g}dx_1dx_2dx_3dx_0 \tag{45}$$

and using the divergence theorem on the flux term, and approximating the spatial integral on the source term;

$$\int_{\Delta x_0} \frac{\partial}{\partial x_0} Q \Delta V^{(3)} dx_0 + \int_{\Delta x_0} \int_{\partial V} f(q) d\Sigma dx_0 = \int_{\Delta x_0} \hat{S}(q) \Delta V^{(4)} dx_0 \tag{46}$$

$\hat{S}(q)\Delta V^{(4)} = \int_{\Delta V^{(3)}} S(q)\sqrt{-g} dx_1 dx_2 dx_3$, $\Delta V^{(4)} = \sqrt{-g}\Delta x_1 \Delta x_2 \Delta x_3$
approximate the integral over the flux terms;

$$\int_{\Delta x_0} \frac{\partial}{\partial x_0} Q \Delta V^{(3)} dx_0 + \int_{\Delta x_0} f^i(q) \Delta \Sigma_i dx_0 = \int_{\Delta x_0} \hat{S}(q) \Delta V^{(4)} dx_0 \tag{47}$$

where $\Delta\Sigma_j = \sqrt{-g} dx_i dx_k \epsilon_{ijk}$ such that the direction of the surface element is orthogonal to the surface area in question.

Now we perform the time integration

$$(Q\Delta V^{(3)})^{n+1} - (Q\Delta V^{(3)})^n + \Delta x_0 \sum_j \Delta\Sigma_i F^i_j(q) = \hat{S}\Delta V^{(4)} \tag{48}$$

where we have defined $F^i(q) = \frac{1}{\Delta x_0}\int_{\Delta x_0} f^i(q) dx_0$, and assumed that the evolution is over such a short period of time that the sources remain constant in time (as with the surfaces through which the flux travels. The sum over j is simply the sum of the fluxes over all cell faces.

Now we have;

$$Q^{n+1} = Q^n - \frac{\Delta x_0}{\Delta V^{(3)}} \sum_j \Delta\Sigma_i F^i_j(q) + \hat{S}\frac{\Delta V^{(4)}}{\Delta V^{(3)}} \tag{49}$$

To handle the flux time integral without explicitly performing the integral, we rely on approximations such as the Roe solver, Tadmor, Marquina, HLLE, HLLC etc...

I explain the Roe solver below, the others mentioned may be found in papers on my references webpage (see bibliography).

In this form, one can handle discontinuities rather easily by breaking up the integrals to integrate over the continuous parts of space. Here is where we implement Godunov's idea. We think of the discritization $Q^n_i$ as being a piecewise constant reconstruction of the solution q(x). Then at every cell boundary we have a Riemann problem (the discontinuity). To estimate the flux in the above equation we write the flux as $f(q^*)$ where $q^*$ is the solution at the cell boundary to the problem given by:

$$\frac{\partial q}{\partial t} + A\frac{\partial q}{\partial x} = 0 \tag{50}$$

where the Jacobian $A = \partial F/\partial q$ is considered constant. Essentially we have linearized the equation. The following refers to the figure 1. From here we want the characteristics of 50 which are calculated by $x - At = k$ for constant k. Thus $q^*$;

For $x = 0$: If $A > 0$ the flow is to the right, so $q^* = q_L$, this corresponds to $f(q^*) = Aq_L$. If $A < 0$ the flow is to the right, so $q^* = q_R$, which corresponds to $f(q^*) = Aq_R$. Rather than using an if/then approach we use a general form:

$$f_{i+1/2} = f(q^*_{i+1/2}) = \frac{1}{2}\left(Aq_L + Aq_R - |A|(q_R - q_L)\right) \tag{51}$$

So if $A > 0$ then $f = \frac{1}{2}(Aq_L + Aq_L) = Aq_L$

# 12 The $\nabla \cdot \vec{B} = 0$ constraint

Regular Riemann solvers, when applied to the magnetic field components, will eventually disobey the magnetic field constraints. This comes about from numerical dissipation, and is of course impossible physically, it exposes flaws in the flux calculations. Several remedies have been investigated. The first was done by Hawley and Evans (1978) using what they called Constrain Transport. The difficulty in their method is that

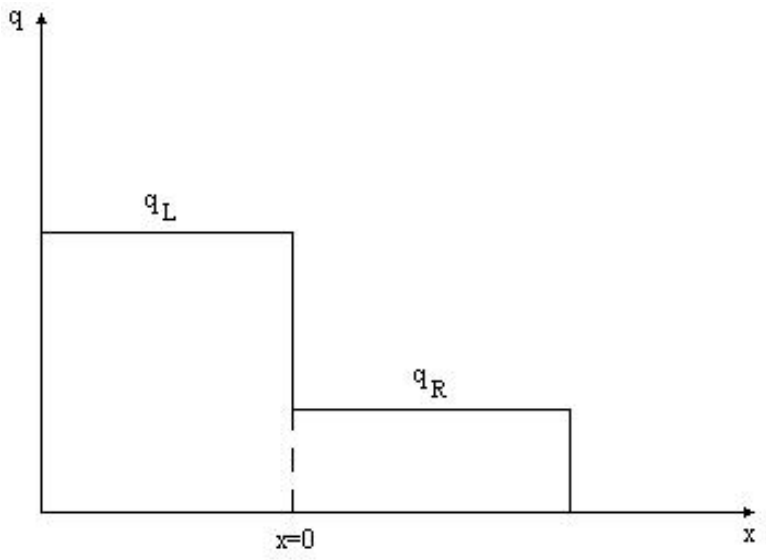


Figure 1: The setup for the Riemann Problem

they use a staggered grid approach where one evaluates the magnetic field components at the face centered locations, and the flux is then to be calculated in the corners. This adds to the computation time, as well as the overall complexity in the implementation of the code. Despite these complications, it persists in being the most reliable method of ensuring the constraint is obeyed.

Later Powell considered reformulating the conservation equations to explicitly include $\nabla \cdot B$ terms. This term is an auxillary variable, and thus evolves with the fluid equations. This method is considered by Gabor Toth (2000). Toth's conclusions were that the constrained transport can be realized using cell centered coordinates and field values. This method involves a flux averaging using neighbouring cells. It is explained very well in "HARM ..." by Gammie et al.

Essentially the idea behind this was to involve two ideas. First we extend the stencil to more grid points in a finite difference style calculation of div B. The second was to calculate an average for the magnetic field flux calculations. This mixes the flux terms for all magnetic field directions, however due to the extended stencil this allows for a complete cancellation of the flux terms. In my experience with this calculation I find the results are around three orders of magnitude more accurate for div B. Details of the mathematics are shown below;

$$\nabla \cdot \vec{B} = 0 \tag{52}$$

in 2D takes on the form

$$\frac{\partial B_x}{\partial x} + \frac{\partial B_y}{\partial y} = 0 \tag{53}$$

In finite difference form

$$\frac{B_x(i+1,j) - B_x(i,j)}{\Delta x} + \frac{B_y(i,j+1) - B_y(i,j)}{\Delta y} = 0 \tag{54}$$

or in an extended stencil

$$\frac{B_x(i,j) + B_x(i,j-1) - B_x(i-1,j) - B_x(i-1,j-1)}{2\Delta x} + \frac{B_y(i,j) + B_y(i-1,j) - B_y(i,j-1) - B_y(i-1,j-1)}{2\Delta y} = 0. \tag{55}$$

Now if we look at the expansion of the magnetic flux term in the Godunov scheme;

$$\partial_t(\sqrt{\gamma}B^k)(i,j) = \partial_l(\sqrt{-g}F^{kl})(i,j)$$

Which became (after FVM treatment)

$$B^{k,n+1} = B^{k,n} - \frac{\Delta x_0}{\Delta V^{(3)}} \sum_i \Delta\Sigma_j F_i^{k,j}(q) \tag{56}$$

NOTE: No source terms are expected on the induction equation (see later in this set of notes)
Let us focus on 2D $i \in [1,2]$

$$B^{k,n+1} = B^{k,n} - \frac{\Delta x_0}{\Delta V^{(2)}} \left(\Delta\Sigma_j F_1^{k,j} + \Delta\Sigma_j F_2^{k,j}\right) \tag{57}$$

$\Delta V^{(2)} = \sqrt{\gamma}dx_1dx_2$

$$B^{k,n+1} = B^{k,n} - \frac{\Delta x_0}{\Delta V^{(2)}} \left(\Delta\Sigma_{x_1R} F_R^{k,x1} - \Delta\Sigma_{x_1L} F_L^{k,x1} + \Delta\Sigma_{x_2R} F_R^{k,x2} - \Delta\Sigma_{x_2L} F_L^{k,x2}\right) \tag{58}$$

where the R and L denote the left and right evaluation of the flux in the cell. $F^{kl}$ represents the flux for the magnetic field.

What is important here is that the approximation $\Delta\Sigma_{x_i} \sim \sqrt{-g}dx_jdx_k\epsilon^{ijk}$ (in 3D) carries a $\sqrt{-g}$ term which is to be evaluated on the surface of the cell interface. Thus it takes on the $R, L$ notation used for the actual flux term. If we group this term in with the flux ie let $\mathcal{F} = \sqrt{-g}F$ then we have;

$$B^{k,n+1} = B^{k,n} - \frac{\Delta x_0}{\Delta V^{(2)}} \left(\Delta x_2 \mathcal{F}_R^{k,x1} - \Delta x_2 \mathcal{F}_L^{k,x1} + \Delta x_1 \mathcal{F}_R^{k,x2} - \Delta x_1 \mathcal{F}_L^{k,x2}\right) \tag{59}$$

Now, to prove something with the constraint, we take the divergence of the above equation. Since we assume the initial conditions are in agreement with the constraint (ie for $n = 0$ we demand that this be true) we expect

$$\partial_k(\sqrt{\gamma}B^k)^n = 0$$

identically. Also note:

$$\partial_0(\sqrt{\gamma}B^k) + \partial_i(\mathcal{F}^{ki}) = 0 \tag{60}$$
$$\partial_k\partial_0(\sqrt{\gamma}B^k) + \partial_k\partial_i(\mathcal{F}^{ki}) = 0 \tag{61}$$
$$\partial_0\partial_k(\sqrt{\gamma}B^k) + \partial_k\partial_i(\mathcal{F}^{ki}) = 0 \tag{62}$$
$$\partial_k\partial_i(\mathcal{F}^{ki}) = 0 \tag{63}$$

Where the last line is true simply due to antisymmetry of the Flux term, and the symmetry of the partial derivatives.

Thus we have that the divergence of the induction equation leads to a new form of the divergence constraint. This form is easily applied to the finite volume method since the fluxes are calculated at the cell interfaces.

Since the integral form of the equation preserves symmetry one expects that taking an average over flux interfaces will also preserve the symmetry.

Multiply the FVM treatment of the variables by the geometric term $\sqrt{\gamma}$;

$$\sqrt{\gamma}B^{k,n+1} = \sqrt{\gamma}B^{k,n} - \sqrt{\gamma}\frac{\Delta x_0}{\Delta V^{(2)}} \left(\Delta x_2 \mathcal{F}_R^{k,x1} - \Delta x_2 \mathcal{F}_L^{k,x1} + \Delta x_1 \mathcal{F}_R^{k,x2} - \Delta x_1 \mathcal{F}_L^{k,x2}\right) \tag{64}$$

Recall that the definition $\Delta V^{(3)} \sim \sqrt{\gamma}dx_1dx_2dx_3$ (in 3D) expanding this in the above expression cancels the "extra" geometric factor introduced with the generalized divergence. We are left with (again focusing on 2D);

$$\sqrt{\gamma}B^{k,n+1} = \sqrt{\gamma}B^{k,n} - \frac{\Delta x_0}{\Delta x_1\Delta x_2} \left(\Delta x_2 \mathcal{F}_R^{k,x1} - \Delta x_2 \mathcal{F}_L^{k,x1} + \Delta x_1 \mathcal{F}_R^{k,x2} - \Delta x_1 \mathcal{F}_L^{k,x2}\right) \tag{65}$$

Now take the divergence of the above equation, keeping in mind that $\mathcal{F}^{ii} = 0$;

$$\partial_k(\sqrt{\gamma}B^k)^{n+1} = \partial_k(\sqrt{\gamma}B^k)^n - \frac{\Delta x_0}{\Delta x_1}\partial_{x_2}\left((\mathcal{F}^{x_1x_2})_R - (\mathcal{F}^{x_1x_2})_L\right) + \frac{\Delta x_0}{\Delta x_2}\partial_{x_1}\left((\mathcal{F}^{x_2x_1})_R - (\mathcal{F}^{x_2x_1})_L\right) \tag{66}$$

Now if we assume $\partial_k(\sqrt{\gamma})^n = 0$ which is demanded for $n = 0$ we are left with

$$\partial_k(\sqrt{\gamma}B^k)^{n+1} = \frac{\Delta x_0}{\Delta x_1}\partial_{x_2}\left((\mathcal{F}^{x_1x_2})_R - (\mathcal{F}^{x_1x_2})_L\right) + \frac{\Delta x_0}{\Delta x_2}\partial_{x_1}\left((\mathcal{F}^{x_2x_1})_R - (\mathcal{F}^{x_2x_1})_L\right) \tag{67}$$

Further defining $\mathcal{B} = \sqrt{\gamma}B$ the extended stencil becomes;

$$\begin{aligned}&\frac{\mathcal{B}_{x_1}(i,j) + \mathcal{B}_{x_1}(i,j-1) - \mathcal{B}_{x_1}(i-1,j) - \mathcal{B}_{x_1}(i-1,j-1)}{2\Delta x_1} + \\ &\frac{\mathcal{B}_{x_2}(i,j) + \mathcal{B}_{x_2}(i-1,j) - \mathcal{B}_{x_2}(i,j-1) - \mathcal{B}_{x_2}(i-1,j-1)}{2\Delta x_2} = 0\end{aligned} \tag{68}$$

Where it is clear that if we group the geometric terms with the dynamic variables $\mathcal{B} = \sqrt{\gamma}B$ we recover the stencil for the cartesian coordinates in Minkowski space. Further noting that the flux terms are really unaffected by the new geometric factor. Thus it appears that the only averaging that needs to be performed in over the $\mathcal{F}$ fluxes and not any geometric terms associated with taking the divergence. (ie do not include an extra factor of $\sqrt{\gamma}$ in the flux terms before averaging.)

Performing the finite difference on the expanded stencil we have,

$$\begin{aligned}\partial_k(\sqrt{\gamma}B^k)^{n+1} = &\frac{\Delta t}{\Delta x}\left[\frac{1}{2\Delta y}\left(\mathcal{F}^{xy}_{i+\frac{1}{2},j} + \mathcal{F}^{xy}_{i-\frac{1}{2},j} - \mathcal{F}^{xy}_{i+\frac{1}{2},j-1} - \mathcal{F}^{xy}_{i-\frac{1}{2},j-1}\right)\right] - \\ &\frac{\Delta t}{\Delta x}\left[\frac{1}{2\Delta y}\left(\mathcal{F}^{xy}_{i-\frac{1}{2},j} + \mathcal{F}^{xy}_{i-\frac{3}{2},j} - \mathcal{F}^{xy}_{i-\frac{1}{2},j-1} - \mathcal{F}^{xy}_{i-\frac{3}{2},j-1}\right)\right] + \qquad (69)\\ &\frac{\Delta t}{\Delta y}\left[\frac{1}{2\Delta x}\left(\mathcal{F}^{yx}_{i,j+\frac{1}{2}} + \mathcal{F}^{yx}_{i,j-\frac{1}{2}} - \mathcal{F}^{yx}_{i-1,j+\frac{1}{2}} - \mathcal{F}^{yx}_{i-1,j-\frac{1}{2}}\right)\right] - \qquad (70)\\ &\frac{\Delta t}{\Delta y}\left[\frac{1}{2\Delta x}\left(\mathcal{F}^{yx}_{i,j-\frac{1}{2}} + \mathcal{F}^{yx}_{i,j-\frac{3}{2}} - \mathcal{F}^{yx}_{i-1,j-\frac{1}{2}} - \mathcal{F}^{yx}_{i-1,j-\frac{3}{2}}\right)\right] \qquad (71)\end{aligned}$$

Finally we use the flux averaging explained in Gammie et al.

INSERT IMAGE FOR FLUX AVERAGING

We have the flux average for all cell boundaries follows the form:

$$\begin{aligned}&{}^*\mathcal{F}^{xy}(i+\tfrac{1}{2},j) = \\ &\frac{1}{2}\left(\frac{1}{4}\left(\mathcal{F}^{xy}(i+\tfrac{1}{2},j) + \mathcal{F}^{xy}(i-\tfrac{1}{2},j) + \mathcal{F}^{xy}(i,j+\tfrac{1}{2}) + \mathcal{F}^{xy}(i,j-\tfrac{1}{2})\right) + \right. \\ &\left.\frac{1}{4}\left(\mathcal{F}^{xy}(i+\tfrac{1}{2},j) + \mathcal{F}^{xy}(i+\tfrac{3}{2},j) + \mathcal{F}^{xy}(i+1,j+\tfrac{1}{2}) + \mathcal{F}^{xy}(i+1,j-\tfrac{1}{2})\right)\right)\end{aligned} \tag{72}$$

Which reduces to:

$$\begin{aligned}&{}^*\mathcal{F}^{xy}(i+\tfrac{1}{2},j) = \\ &\frac{1}{8}\left(2\mathcal{F}^{xy}(i+\tfrac{1}{2},j) + \mathcal{F}^{xy}(i-\tfrac{1}{2},j) + \mathcal{F}^{xy}(i-\tfrac{1}{2},j)\right. \\ &\left.-\mathcal{F}^{yx}(i,j+\tfrac{1}{2}) - \mathcal{F}^{yx}(i,j-\tfrac{1}{2}) - \mathcal{F}^{yx}(i,j+\tfrac{1}{2}) - \mathcal{F}^{yx}(i,j-\tfrac{1}{2})\right)\end{aligned} \tag{73}$$

likewise for ${}^*\mathcal{F}^{yx}(i,j+\frac{1}{2})$

Using Maple I verified that these two expressions are identically zero, thus we remove the magnetic field constraint violations that occur due to the evolution.

Another method is known as elliptic cleaning where the magnetic field is re-written as $B' = B + \nabla\phi$, and the constraint to be fixed is $\nabla \cdot B' = 0$. This leaves an elliptic problem for $\phi$ with $\nabla \cdot B$ as a source term. The next step is to update the magnetic field $B'$, and use this for the next time step evolution. The disadvantage of this method is that is it computationally expensive. To circumvent this difficulty it is recommended that elliptic cleaning not be performed on every time step.

# 13 Boundary Conditions

The finite volume method as described above works well in the body of a domain. The trouble comes near boundaries of the domain where one cannot easily perform the flux averaging between adjacent cells. To remedy this, I use extra cells around the main domain, common referred to as ghost cells. How one updates these cells will depend on the physical setup of the problem at hand. Typically the boundary updates will be one of, or a combination of, the following:

- Periodic BC's - simply match the values of the ghost cells to the values of opposite side of the domain. This is a straightforward copy. Applications of this boundary come from an infinite domain, or if using spherical coordinates, keeping the domain between 0 and $2\pi$
- Simple Outflow BC's - one copies the values on the edge of the domain into the ghost cells. Again a straightforward copy.
- Inflow BC's - one has some initial value for the edge of the domain, and after every time step one uses that original value in the place of the ghost cell. This is also known as a prescribed boundary condition. Physically this corresponds to inflowing matter into the domain, commonly used in jet simulations.
- Reflective - Takes advantage of symmetry in the system, takes the values of the cells next to the ghost cells and copies all those except for the vector quantities. The vector quantities parallel to the boundary are also simply copied. Vector quantities perpendicular to the boundary are negated.
- Extrapolated outflow - one uses the values in the cells next to the boundary to extrapolate the expected values in the ghost cells. This is used to prevent artificial reflections that may occur when using the simple outflow BC's. Depending on the physical setup this condition may or may not be used. Caution must be used here, since sometimes the extrapolation of either the density or the pressure may allow ghost cell values to drop below tolerance levels or become negative. This can lead to flux values that cause the system to fail.

These prove to be sufficient for many different physical setups, including the Bondi-Hoyle-Lyttleton accretion problem setup in this project.

The standard boundary conditions for a PDE system are Dirichelet and Neumann. Dirichelet conditions hold the points along the boundary as constant in time. Consequently performing a volume integral over the boundary cells leads to another constant. This leads to the inflow boundary condition. The Neumann condition holds the normal derivative at the boundary constant in time. A volume integral over this leads to the outflow boundary condition.

The periodic BC and the reflective BC may be considered as mechanisms to avoid boundaries. Periodic BC imply an infinite domain. Reflective can be used in cases where there is a symmetry in the problem and calculations are redundant over the entire domain. This is useful in axisymmetry. The other case where reflective boundary conditions are useful is when we experience a solid wall.

It is also noted that characteristics near physical boundaries will determine the need for a boundary condition. If the boundary condition used constradicts the characterists along that boundary, the resulting calculation will be meaningless.

# 14 Jacobian and Eigenvalues

We have discussed characteristics and their value for solving the PDE's, now we turn to their values and physical meaning. From Font etal. we have explicit calculations for the eigenvalues for the Jacobian matrices for ideal MHD. I list the results for the $i$th-direction waves:

The matter wave

$$\lambda_M = \alpha v^i - \beta^i$$

The Alfven wave

$$\lambda_{a\pm} = \frac{b^{x_1} \pm \sqrt{\rho h + b^2} u^i}{b^t \pm \sqrt{\rho h + b^2} u^t}$$

The magnetosonic waves are the solutions to a fourth order polynomial

$$N_a = \rho h \left( \frac{1}{c_s^2} - 1 \right) a^4 - \left( \rho h + \frac{b^2}{c_s^2} \right) a^2 G + B^2 G = 0$$

with

$$a = \frac{W}{\alpha} \left( -\lambda + \alpha v^i - \beta^i \right)$$

$$B = b^i - b^t \lambda$$

$$G = \frac{1}{\alpha^2} \left( -(\lambda + \beta^i) + \alpha^2 \gamma^{ii} \right)$$

and $c_s$ is the speed of sound.

This accounts for 7 of the 8 expected wave velocities. The last wave velocity is expected to be zero, since the magnetic field contributions from the direction in question are non-existent. (IE the $B^i$ contributions in the x-direction do nothing)

An important note is that the above code calculations require the use of the given flux variables, the conservative definitions and the 3+1 decomposition functions, so to find these eigenvalues we have:

the conservative variables $F^0$, the flux contributions $F^i$, and the primitive variables $P$, as a generalized eigenvalue problem

$$A_0 = \frac{\partial F^0}{\partial P}$$

$$A_1^i = \frac{\partial F^i}{\partial P}$$

$$A_1^i \vec{q} = \lambda \alpha A_0 \vec{q}$$

Note in numerical routines, typical eigenvectors returned need to be multiplied by the $A_0$ matrix to return the eigenvectors to the overall system.

Also note that although the papers I cite use a Jacobian that includes the lapse function, one can simply multiply the resulting eigenvalues by this lapse if critical. The flux calculation I consider does not include this extra term.

# 15 Iterative Procedure

One of the more challenging problems facing GRMHD was the recovery of the primitive variables. In the Newtonian code these are known in closed form however due to the lorentz factor we are left to use an iterative procedure for the recovery in this system. I will give a brief outline of Del Zanna's 1D conservative to primitive variable solver here. For more details please see his paper. The author is aware of the Noble paper that discusses several techniques. This method is straight forward and quick enough to implement for now.

We set $\Omega = \rho h \gamma^2$, and $Q = \gamma_{ij} S^j B^i$

Then we have a new form for the energy equation

$$\tau = E - D = \Omega - P + \left( 1 - \frac{1}{2W^2} \right) |B|^2 - \frac{Q^2}{2\Omega^2} - D \tag{74}$$

and the momentum equation

$$|S|^2 = (\Omega + |B|^2)^2 \left(1 - \frac{1}{\gamma^2}\right) - \frac{Q^2}{\Omega^2}(2\Omega + |B|^2) \tag{75}$$

Re-writing the momentum equation we solve for $W$

$$W = \left[1 - \frac{Q^2(2\Omega + |B|^2) + |S|^2\Omega}{(\Omega + |B|^2)^2\Omega^2}\right]^{-\frac{1}{2}} \tag{76}$$

We replace the pressure term using the equation of state:

$$P(\Omega) = \frac{(\Omega - DW)(\Gamma - 1)}{\Gamma W^2} \tag{77}$$

Finally we can start using Newton's procedure using the energy equation

$$f(\Omega) = \Omega - P + \left(1 - \frac{1}{2W^2}\right)|B|^2 - \frac{Q^2}{2\Omega^2} - D - \tau = 0 \tag{78}$$

and we require the first derivative

$$\frac{df}{d\Omega} = 1 - \frac{dP}{d\Omega} + \frac{|B|^2}{W^3}\frac{dW}{d\Omega} + \frac{Q^2}{\Omega^2} \tag{79}$$

with

$$\frac{dP}{d\Omega} = \frac{\left(W\left(1 + D\frac{dW}{d\Omega}\right) - 2\Omega\frac{dW}{d\Omega}\right)(\Gamma - 1)}{\Gamma W^3} \tag{80}$$

$$\frac{dW}{d\Omega} = -W^3\frac{2Q^2\left(3\Omega^2 + 3\Omega|B|^2 + |B|^4\right) + |S|^2\Omega^3}{2\Omega^3\left(\Omega + |B|^2\right)^3} \tag{81}$$

Solving this with an initial guess of $\Omega = 500$ appears to work well for all cases (ultra relativistic, zero velocity, moderately relativistic,and Newtonianesque).

With the value of $\Omega$ determined we can solve for the primitive variables. This is done by re-arranging the above expressions, and of course using the last value of $\Omega$ obtained.

$$v_k = \frac{1}{\Omega + |B|^2}\left(S_k + \frac{Q}{\Omega}B_k\right) \tag{82}$$

$$P(\Omega) = \frac{(\Omega - DW)(\Gamma - 1)}{\Gamma W^2} \tag{83}$$

$$W = \left[1 - \frac{Q^2(2\Omega + |B|^2) + |S|^2\Omega}{(\Omega + |B|^2)^2\Omega^2}\right]^{-\frac{1}{2}} \tag{84}$$

$$\rho_o = \frac{D}{W} \tag{85}$$

Note that the magnetic field components are unaltered. They are both primitive and conservative variables.

# 16 The Floor, and other numerical restrictions

For relativistic fluids one is in consistent danger of producing either negative pressures (usually arising from negative energy) or negative baryon densities. To circumvent this issue we use a numerical floor. This floor is typically imposed on the conservative variables, before calculating the primitives. What seems to be the case is that different floors can be used on the energy than the baryon density, by a few orders of magnitude. Several authors have investigated this behaviour and found that the floor used in the hydrodynamic code (on order of $10^{-11}$ or smaller) had little effect on their results. For the MHD case the problem is a little more apparent due to the contribution from the magnetic field (obviously I suppose), McKinney et al. investigated this problem in their paper (2006 - include in references), and found that the floor is a little more restrictive, on the order of $10^{-7}$. Specifically in this paper they also made the floor dependent on the radial distance from the origin, with significant justification. Further, they found that this floor had little bearing on the computed results. The method of floor decided upon, after a discussion with Neilson, was to determine a maximum between a floor value and the Conservative density, or the Energy. Later checking to ensure the primitive density and pressure are greater than floor or set equal to floor. Finally if the primitive variables were altered the conservative variables are recalculated to ensure self consistency.

Author's note: It is important to understand that the floor is not a physical quantity, but rather a numerical control. It has been observed that this quantity is only necessary in what are considered ultrarelativistic velocities. (very close to the speed of light) In astro papers one must watch out for the language used. In several papers they refer to superluminal speeds, which is the same as saying ultrarelativistic as defined above, in GR type journals superluminal appears to commonly mean "exceed the speed of light".

Numerical techniques may also lead to non-zero values where one clearly expects proper zero. Of course this usually corresponds to rounding errors, and lack of "infinite precision", (such as trying to calculate $\cos \pi/2 = 0$ for a numerical value of pi). This can cause catastrophic effects when trying to perform such tasks as inverting matrices, and trying to calculate a Newton Iterative procedure. The need for a tolerance parameter originally arose when inverting matrices to calculate the eigenvectors for the Roe approximation in the MHD code. The close to zero values which were well distributed in the matrix (near zero meaning $\sim 10^{-16}$), which when inverting the matrix returned extremely high values ($\sim 10^{200}$) which of course are incorrect. Further inspection indicated that theoretically these small values were zero, but numerically these were "essentially" zero, or at least below machine precision. The introduction of a tolerance parameter to replace the "essentially zero" elements with exactly zero elements, did the trick. This does lead to some troubling concerns, however investigation upon investigation reveals that this tolerance parameter has no effect on the results, unless of course it is too liberal in defining zero, or strict beyond machine precision (in which case the computer will never use the tolerance anyways). I found that an acceptable value of tolerance is around $10^{-13}$. This means that the resolution of the results is unknown below this tolerance, however as more numerical techniques are developed, and the precision of the standard compilers (right now 32bit is the standard) increases this tolerance should diminish and ideally zero tolerance will be reached.

As mentioned the tolerance is also useful for defining a limit on the Newton-Raphson solver. This tolerance can be played with a little, and could in principle be reduced below the precision of the matrix tolerance. There is some advantage to this, first it ensures that the matrix tolerance is the limiting precision. Secondly it has been experimentally verified (by this author) that the lower this tolerance is the more likely the primitive variable solver will return non-superluminal velocities. This is accomplished by scaling the tolerance by a few orders of magnitude as it is applied to the solver. One does have to be careful since if tolerance is too low, one can get trapped in the Newton solver forever.

# 17 Equation of State

The given MHD equations do not form a closed set, to further specify the system we are required to select an equation of state. $P \rightarrow P(\rho, s)$. Strictly speaking most of the field is concerned with isentropic systems, so the EoS reduces to $P \rightarrow P(\rho)$. For the relativistic gases I chose the ideal gas $P = (\Gamma - 1)\rho_o\epsilon$, and $h = 1 + \epsilon + \frac{P}{\rho_o}$.

For the temperature dependent EoS, one may take, as a trivial example, the ideal gas EoS;

$$PV = nkT \rightarrow P = \rho_o kT,$$

where $T$ is the temperature of the gas. Keeping with tradition I shall use geometric units here too ($k \to 1$). Given this one must concern themselves with the compatibilities between the ideal gas and ideal fluids. With this we see that the temperature of an accretion disk is simply the ratio of the pressure to the baryon density, and may be calculated after the evolution has been completed. One must keep in mind Taub's work on this, where there is some inequality for the EoS, and if this is violated the results are physically meaningless. More complicated EoS may be necessary. McKinney et al, followed this path and discovered that it may be possible to expand the ideal gas EoS such that the $\Gamma$ is a variable. They found an approximation to Taub's Bessel function of the second kind formulation of the EoS. It does not appear that the literature has caught on with this new form of the EoS and they may have a good reason to ignore this, or it could be that they are simply more interested in other features of the accretion disk and are not quite ready for the headache of an extra parameter.

In keeping in line with the literature I will use both the traditional EoS and to advance things a little, the one proposed by McKinney et al. Aside from that, if I want to include a stiffness term I can add a base pressure (constant) and keep things physical. There will be more on this later if I see the need.

# 18 Dimensionless Parameters

In hydrodynamics we are faced with several dimensionless parameters such as:

- Reynolds Number
- Prandtl Number
- Mach Number
- Knudsen Number
- Richardson Number
- Strouhal Number

The Reynolds Number is the ratio of the mean fluid velocity, the characteristic Length (cross section, or domain size). In the ideal MHD systems the Reynolds number tends to infinity, so the fluid viscosity is considered to be zero.

The Prandtl number is the ratio of the momentum of diffusivity and the thermal diffusivity. In ideal fluids the Prandtl number is not a factor in the system, since momentum diffusivity is zero. However as we deviate from the ideal fluids this number needs to be kept in mind.

Mach number is the ratio of the velocity of the fluid and the speed of sound in the fluid. This is a measurable observable.

Knudsen number is the ratio of the mean free path and the length scale of the fluid. This length scale could be the diameter of the fluid body (whatever length scale is used for the Reynolds number calculation must be used here). The Knudsen number determines whether continuum mechanics or statistical mechanics dominates for a fluid. In our case the Knudsen number is small since we are assuming tightly packed particles. If this is violated, say in a situation where pressure and density are both far too low, the MHD approximation will breakdown and the results are no longer reliable.

For an ideal gas the Knudsen number may be calculated by

$$Kn = \frac{kT}{\sqrt{2}\pi\sigma^2 PL}$$

where $kT$ is the thermal energy, $\sigma$ is the particle diameter (very small in SI units), P is the pressure, and L is the length scale. The length scales in the problems at hand are quite large, on the order of 100 AU ($15x10^{12}$). k is very small ($1.38x10^{-23}$), which leaves us with a wide range of allowable temperature to pressure ratios which will still be valid in the continuum limit. (I dropped the units since the equation is well known, and all I care about is scaling.

Richardson number is the ratio of the gravitational potential energy to the fluid kinetic energy. Since in our case I treat gravity through the geometry I do not include a source term representing gravity. This number is thus also treated as zero.

Strouhal number is used to measure the oscillating flow of the fluid around some obstacle in the trajectory., Again, since I have not implemented any obstacles, this number is of little value. In the future development of code, I will reconsider this number if I allow for larger objects to pass through the accretion disks.

Likewise magnetohydrodynamic systems have dimensionless parameters:

- Magnetic Reynolds Number
- Beta
- Alfven Number

The magnetic Reynolds number is the ratio of the characteristic velocity times the length scale, with respect to the magnetic diffusivity (inversely proportional to the conductance). In our case the magnetic Reynolds number is infinite, so the diffusive terms are negligible. Astrophysically this has been observed to be true in extreme cases.

The $\beta$ is the ratio of the magnetic pressure and the hydrodynamic pressure. This is a measurable observable.

The Alfven number is the ratio of the Alfven speed to the characteristic speed of the system. This is also a measurable observable.

# 19 Coordinates and Grids

Typically we have two decent choices for grids in the stationary metric setup. The regular grids wherein the points are spaced at equal intervals. For the cases where one has singularities in the geometry, such as in the case of the Schwarzschild metric. In this case one wants to have more grid points located near the horizon. (As opposed to the slightly more complicated procedure of changing the metric) To do this one can select the logarithmic coordinate. I will describe the coordinate production procedure soon. The procedure was simply to take the range between 1 and 10, divide it into $n$ parts, (n being the number of cells). Then taking the log of each division, treat each of those as a percentage. use this percentage to determine where the next grid point lands on any given physical domain. This technique, if done properly, will result in a higher density of grid points near one edge of the domain.

To start this process I use the standard special relativistic metric expressed in cartesian coordinates. There is little more to say on this matter, the metric is constant, diagonal, and we have trivial lapse and shift. The particulars of the metric will be expressed in the appropriate section below. To try to generalize things I switch to a curvilinear representation, this makes the lapse non trivial and the metric itself is no longer constant.

Moving along, I went to the Schwarzschild coordinates for a Schwarzschild black hole. There are known singularities in this coordinate system at $r = 2M$. Since this is known to simply be a coordinate singularity one can invent a new set of coordinates to circumvent this issue. These were found by Kruskal and Szekeres. There are two types of these coordinates, ingoing with $v = t + r^*$ and outgoing with $u = t - r^*$ where

$$r^* = \int \frac{dr}{1 - 2M/r} = r + 2M \ln \left| \frac{r}{2M} - 1 \right|$$

We see in the singularity has been absorbed into the definition of the new radial coordinate. The full set of Kruskal coordinates can be used to cover the entire spacetime; however, has been found that these coordinates are "awkward" to work with, and that one does not necessarily need to work with the entire spacetime diagram. It is sufficient to cover the sections of spacetime that lead to the future null horizon. (Most of this comes from Eric Poisson's book)

The next physical situation that needs to be addressed is a non-static black hole. I turn to the Kerr solution. Unfortunately this coordinate while expressed in Schwarzschild coordinates lead to singularities on a few locations in spacetime. To remedy this we turn to a generalized version of the Eddington-Finkelstein

coordinates known as the Kerr-Schild coordinates. These coordinates allow us to separate the metric into two pieces, one in which we have the flat spacetime metric, the other being all the angular momentum terms.

From Hawking and Ellis we have a simple relation between the Kerr–Schild coordinates and the Boyer–Lindquist coordinates.

$$\begin{aligned} x + iy &= (r + ia)\sin\theta e^{i\psi} && (86)\\ z &= r\cos\theta && (87)\\ t' &= v - r && (88) \end{aligned}$$

In following matter into the future black hole we use the ingoing null coordinates. This leads to a mixing of the radial and temporal coordinates.

The typical grid choices for this type of work are a logarithmic grid over the radial coordinate, and a regular grid over the angular domain. One expects, depending on the coordinate choice, a need for higher accuracy near the event horizon. For simplicity I select a logarithmic grid over a logarithmic coordinate. Although, through the work of Font etal. we have seen that horizon adapted coordinates make for a much better choice. They allow one to work right up to and inside of the event horizon. This means that one truly can apply the outgoing boundary condition at the inside boundary, without the concern that arises when one artificially sets a boundary on the outside of the event horizon. Researchers have found that the artificial boundary outside of the event horizon leads to numerical reflections, and consequently needs to be damped. The use of a logarithmic grid allows one to have more grid points near the event horizon without changing the metric. This was useful for code development where changing the metric leads to too many changes occurring simultaneously and untractable errors creeping up.

# 20 Trials

## 20.1 1 Dimensional Problems

### 20.1.1 Riemann Shock Tubes

A critical test of a finite volume method includes ensuring that shocks are captured. This involves investigating the Riemann shock tube. For the following test we use the Minkowski spacetime. The setup is as follows, the domain is split into two halves, one half has a set of initial conditions (list them), the other has a different set. The setup can go in several different directions, depending on the values of the initial sides. One can setup a Shock-Shock test, a Rarefaction-Shock test, and a Rarefaction-Rarefaction test. If the code breaks down for any of these tests one can immediately realize the limitations of the methods used. Different flux calculations allow for different smoothing of the expected wavefronts. (INSERT IMAGES OF THESE TESTS IN CARTESIAN AND SPHERICAL COORDS)

### 20.1.2 Spherical Accretion

This is a problem originally investigated by F. Curtis Michel in 1971. One considers a steady state fluid system, thus we can ignore the time derivatives. Furthermore we assume that the flow has only a radial dependent. We then concentrate on the resulting ODE's which are solvable in closed form, if we provide an equation of state. The original analysis solved the system down to two integration constants, then used information about the fluid variables at infinity to solve for the values of these constants. Alternative solutions to the constants are given if one uses the fluid properties at critical values, this was performed by Smarr, Hawley etal (later by Gammie et all in HARM). Given some adiabatic index, and either the fluid properties at the critical values one can solve for the effective temperature to calculate the steady state for the system. To determine the quality of the code, one sets up the problem as done in Smarr etal, where one keeps the outer boundary fixed at the value of the final state for all variables, and sets the rest of the domain to some insignificant value. (I set mine down to the order of $10^{-13}$ and the code worked fine.) Then after a transient time the fluid variables are expected to settle to the steady state. If this steady state is not reached there must be a problem with some aspect of the code. In my tests I investigate both the non-magnetized problem.

The fluid in the body of the domain will flow toward the black hole, while being fed by the incoming matter at the outer boundary. Since we expect that fluid will flow towards the hole, and the coordinates are chosen such that they increase away from the hole, the fluid will have a negative velocity with respect to the hole. That being said, the original setup by Michel only solves for the square of the critical 4-velocity. If one selects a positive critical 4-velocity we get a profile that would physically suggest that the fluid is flowing away form the black hole. If instead we select a negative critical 4-velocity the outer boundary will support inflow of matter from outside the domain. This is far more acceptable than the critical values allowed in the Smarr paper. It appears that other authors caught onto this in later papers such as Anton etal (2006) and Del Zanna etal.(2007)

(INSERT PICS of regular grid, log grid and convergence tests. Also include time derivative plots) The results are available on my webpage http://laplace.physics.ubc.ca/People/ajpenner/movies/movies.html

This tests the capability of handling a curved spacetime with as few new parameters as possible. Essentially it proves to be a good test of the lapse function (the only significant change in the code).

A final observation for the hydrodynamic code is that this initial condition proved to be a valuable test for the outflow boundary conditions. If one uses the simple copy neighbouring cell techniques the evolution takes an ugly turn when the radial velocity reflects back from the event horizon due to the high pressure and density. The extrapolated outflow BC prevents sharp unphysical reflections from occurring at this boundary. The rest of the variables do not have an adverse reaction when I use the simple copying neighbouring cell BC. This is exactly what was predicted in the Anton paper.

According to Anton (3+1 characteristic paper) one can impose a radial magnetic field on the spherical accretion and obtain a steady solution.

In the magnetized flow a radially dependent magnetic field is imposed.

First we ensure that the magnetic field will be divergence free. Thus we solve the ODE

$$\partial_r \left(\sqrt{\gamma}\mathcal{B}^r\right) = 0$$

Which results in

$$\mathcal{B}^r = \frac{C}{r^2}$$

where $C$ is an integration constant which is known when we look at the value of $\mathcal{B}^r$ at the critical radius.

Parameterize the magnetic field with the plasma beta function, we can get a magnitude for the magnetic field:

$$\beta = \frac{b^2}{2P} \tag{89}$$

Given $b = (b^t, b^r, 0, 0)$ we have

$$b^2 = g_{tt}(b^t)^2 + g_{tr}b^t b^r + g_{rr}(b^r)^2 \tag{90}$$

To begin I stick with the Schwarzschild metric in Schwarzschild coordinates therein $g_{tr} = 0$ and life is ever so much easier.

To determine the magnitude of the magnetic field at the critical point, and thus solve for $C$:

$$2P_c\beta = \left(1 - \frac{2M}{r_c}\right)(b^t)^2 + \left(1 - \frac{2M}{r_c}\right)^{-1}(b^r)^2 = \left(1 - \frac{2M}{r_c}\right)(B^r)^2 \tag{91}$$

This is not a physical problem. Anton etal. describe in detail why one cannot have a one dimensional force free radial magnetic field. Further closed form analysis of the system of equations shows that including the magnetic field of this kind does not change the setup. The energy is shifted by exactly the magnetic field energy, so no dynamical energies are expected. The momentum itself is unaltered. The energy flux expression is unaltered, and the radial momentum flux is balanced by the source term in the same expression. This test is good for verifying that magnetic field flux calculations are reasonable. It further exposes the limitations of a numerical code's capability in handling the no magnetic monopole contraint in the case where one experiences large magnetic fields.

The significance of this IC not being dynamic is that unlike the purely hydrodynamical case we cannot start with a near vacuum and expect to obtain a steady state solution. The magnetic field itself does not evolve since the flux is identically zero.

The results are available on my webpage
http://laplace.physics.ubc.ca/People/ajpenner/movies/movies.html

The magnetic flux is theoretically expected to be zero for this case. Therein this test is far more useful in the process of developing a magnetic flux reconstruction method than anything else. The use of any of the flux averaging techniques can lead to non–zero magnetic field flux in the radial direction. So strictly speaking any reasonable scheme applied to the 1D case will work, so until this is applied to a system with higher dimension it is not completely satisfying that a flux averaging scheme will work as expected.

### 20.1.3 Ingoing Eddington Finkelstein Coordinates

This coordinate choice for a spherically symmetric black hole allows one to cross the event horizon. Consequently one no longer has to concern themselves with small mesh sizes around the event horizon with the hope that one can obtain information close to the even horizon where a lot of open question about accretion exist.

We re-investigate the steady state accretion problem in the new coordinates. Fortunately after investigation very little changes in the original equations. The solution for the time component of the 4-velocity is a slightly more complicated root, and does have one solution that is singular at the event horizon (the other solution is the physically acceptable one) and the velocity of the fluid at the event horizon no longer tends to infinity ($u_t \neq 1$).

This new coordinate followed a similar analysis to the previous case, allowing the solution to converge to steady state from the correct form of the outer boundary condition. The inner BC is still set to outflow, extrapolation for the radial velocity, and simple outflow for the rest.

This test allows us to ensure the shift function is properly implemented throughout the code. I kept the same critical radius and adhere to the conditions setup in the Smarr paper. Although the final result is not as visually stimulating as later papers it gets the job done.

## 20.2 Convergence

I now turn to investigate convergence properties and independent residuals. Convergence was found to exist if one measures $\frac{\|u^{4h}-u^{2h}\|}{\|u^{2h}-u^{h}\|} = h^n$ where u is one of the fluid variables, $\|\cdot\|$ denotes the $L_2$ norm, and n is the order of convergence. In this test one notices that for the transient time, where the system is leaving the pseudo vacuum state the overall system is only first order. However at later times when the system has stabilized, the expected solutions tends towards the second order solution is obtained between the maxima and the critical point. Since we used a peicewise linear reconstruction, a system with discontinuities or near maxima will only be first order accurate. This effects the overal convergence of the method, which means reaching a true second order convergence in the whole evolution is not possible.

### 20.2.1 Independent residual

Before analysis can be performed on two dimensional codes one needs to verify that the code being used is solving the problem you think it is. Verification that your solver is setup properly is critical to any solution. To do this I setup an independent residual type solution for my problem. To do this one constructs a new approximation to the system of equations. Then one uses the values obtained by the FVM in both the current and previous timesteps. As the system increases in resolution one expects the independent residual to converge to zero. The order of convergence of this test determines the order of convergence for the overall system.

### 20.2.2 Equatorial Accretion in Kerr Metric

The lapse and the shift functions come into play here. This test is based on the method developed by Takahashi etal (from Zanna's ECHO paper). Gammie came up with good values to test, and this was later investigated in closed for by Li (CITE). The expectation is that the accretion disk is stable due to both fluid pressure and magnetic field pressure.

## 20.3 2 Dimensional Problems

### 20.3.1 Minkowski Spacetime Background in Cartesian Coordinates

For this spacetime we have the line element:

$$ds^2 = -dt^2 + dx_1^2 + dx_2^2 + dx_3^2 \tag{92}$$

so the metric takes on the standard special relativistic form $\eta_{\mu\nu}$, this makes quick work of our equations as seen below. The lapse function is unity ($\alpha = 1$), and the shift vector elements are all zero $\left(\beta^i = 0\right)$. Thus 3+1 is fairly straight forward in this spacetime. Further $\sqrt{-g} = \sqrt{\gamma} = 1$, and the Christoffel symbols are zero.

We get the conserved quantities:

$$q = \begin{bmatrix} D \\ S_j \\ \tau \\ B^k \end{bmatrix} \tag{93}$$

along with these one gets the corresponding flux terms:

$$f(q) = \begin{bmatrix} Dv^i \\ S_j v^i + P\delta_j^i - \frac{b_j B^i}{W} \\ \tau v^i + P v^i - (B^j v_j) B^i \\ b^k v^i - v^k b^i \end{bmatrix} \tag{94}$$

There are no source terms in the case of Cartesian coordinates.

With this case I was able to produce turbulence given periodic boundary conditions and with help from Jim Stone's website. I was able to commit to several test initial conditions such as the rigid rotor, the blast wave. All of which were originally produced for Newtonian MHD. The tests used toth's flux averaging technique.

The results are available on my webpage

http://laplace.physics.ubc.ca/People/ajpenner/movies/movies.html

There were a few interesting developments when including the magnetic field. The first and most leading was in the rigid rotor test, and included an initially constant magnetic field in one direction (here the $B_x$ direction). One could easily observe the flattening of the rotating fluid, a dramatic display of the effects the magnetic fields.

Primarily this was intended to be a test setup, however there are several known problems with unknown solutions for which the SRMHD code is sufficient to test.

The relativistic Kelvin-Helmholtz instability was implemented. This instability works in a simple way. We setup two different density fluids, say the middle of the domain are high density, and the remainder a low density fluid. The different density portions are flowing in opposite directions. In my initial setup the velocities were $\pm 0.5c$ and the pressure is initialized as uniform. The boundary conditions applied to this problem are periodic in all directions. Following Stone's Newtonian approach I introduce a random seed in the velocity to stimulate the instability. The amplitude of the seed must be small in comparison to the magnitude of the original field. (IE a perturbation) Now, since we are dealing with a relativistic system, these small perturbations, if random, will lead to rapid shocks. These rapid shocks can be quite harmful to a numerical evolution, and since they are only there to push the system I replace them with a periodic perturbation, keeping tabs on the wavelength. (If too short I deal with a similar shock formation as in the random case.) Once implemented the turbulent areas were predictable (always occurred in the same location). This proved to be a good test best to ensure that my relativistic code is fully capable of capturing the extreme shocks that develop from a naturally evolving system. A random seed may have worked if the amplitude was small enough, or if the seed were randomly placed, not set at every location. Also note that the seed was used for both velocity directions.

The results are available on my webpage (no magnetic field)

http://laplace.physics.ubc.ca/People/ajpenner/movies/movies.html

I include a non-zero magnetic field. The most noticeable effect was a difficulty in generating turbulence. As with the blast spiral the introduction of a magnetic field suppresses natural torques or vorticities that

arise in the evolution. Now the fun with the magnetic fields, is that the setup for the initial conditions may increase or decrease the setup if I choose to not implement a cross magnetic field. (Stone's online examples implement a constant magnetic field in a particular orientation (either x or y).)

The results are available on my webpage (magnetic field)

http://laplace.physics.ubc.ca/People/ajpenner/movies/movies.html

There are several other interesting tests for the Newtonian codes; however, many of the more interesting simulations involve a gravitational acceleration and are best suited for the GR codes.

Another test case that has been well established is the spherical blast wave. This IC is setup such that there is a high density and pressure in a small region of space where it linearly drops to the low pressure and density region surrounding the central disturbance. Further the initial setup of the high density region is that it is rotating in one direction or the other (quite arbitrary). The boundary conditions applied here were outflow in all directions. When the evolution starts the high density region naturally flows into the lower density region, the flow pattern is symmetric. Lobes appear to form, which I attribute to the mesh size. Since one can only approximate a circle on a cartesian computational grid. Higher resolution tests should verify or crush this idea.

Now if we include a magnetic field in a particular direction say, along the y-axis, the fluid loses the symmetry of the lobes. The resulting fluid flow shows a suppression along one axis. This clearly displays the suppressive nature of including magnetic fields. The behaviour of the magnetic field while imbedded in the fluid shows a natural tendency to align to minimize the energy of the system.

### 20.3.2 Minkowski Background in Spherical Coordinates

Before moving on to the Kerr metric I implement the curved coordinates, well that is to say, generalized coordinates. This will allow the shift and lapse functions to take on the same values as in the flat space however there are geometric terms that have to come into play. This was by-in-large more of a simplifying step in code development than anything ground breaking. But as expected in the SRMHD code this may be useful for the development of routines to check conserved or convergent quantities.

$$ds^2 = -dt^2 + dr^2 + r^2 d\theta^2 + r^2 \sin\theta^2 d\phi^2 \tag{95}$$

For simplicity I look at $\theta = \pi/2$, the equatorial plane,

$$ds^2 = -dt^2 + dr^2 + r^2 d\phi^2 \tag{96}$$

. The Christoffel symbols are not all zero in general.

From here we get the conserved quantities:

$$q = \begin{bmatrix} D = \rho W \\ S_i = (\rho_o h + b^2) W^2 v_i - b^t b_i \\ \tau = (\rho_o h + b^2) W^2 - (P + \frac{1}{2} b^2) - (b^t)^2 - D \\ B^k = B^k \end{bmatrix}$$

We are then left with the following flux vector elements:

$$f(q) = \begin{bmatrix} Dv^i \\ S_j v^i + P\delta^i_j - \frac{b_j B^i}{W} \\ \tau v^i + P v^i - \frac{b^t B^i}{W} \\ B^k v^i - v^k B^i \end{bmatrix} \tag{97}$$

And the source terms

$$\Sigma(q) = \begin{bmatrix} 0 \\ T^{\mu\nu} \left( g_{\nu j,\mu} - \Gamma^\lambda_{\mu\nu} g_{\lambda j} \right) \\ -\Gamma^t_{\mu\nu} T^{\mu\nu} \\ 0 \end{bmatrix} \tag{98}$$

Where the Christoffel symbols are close to trivial.

Although, due to symmetry considerations, this can reduce to a 1D problem, it allowed for a more robust test of the code since the two dimensions considered in this problem (r,$\phi$) were not interchangeable as they are in cartesian coordinates. This also leads the way to code development towards solving the Bondi-Hoyle accretion problem.

I have performed a Reimann shock tube test, however since the effect is expected to decay as the wavefront moves radially inward, it is difficult to gauge any measurable effect. Consequently this was just an exercise in code development.

### 20.3.3 Schwarzschild Spacetime Background

For the Schwarzschild spacetime in spherical coordinates we have the line element:

$$ds^2 = -\left(1 - \frac{2M}{r}\right) dt^2 + \left(1 - \frac{2M}{r}\right)^{-1} dr^2 + r^2 d\theta^2 + r^2 \sin^2\theta d\phi^2 \tag{99}$$

$M$ is the mass of the static object in geometric units. This metric contains the well known singularities at the origin and the event horizon $R = 2M$. Clearly this will become an issue in the future, however if one avoids the event horizon, this provides the simplest metric which has a nontrivial lapse, and a trivial shift.

From here we get the conserved quantities:

$$q = \begin{bmatrix} D = \rho W \\ S_i = (\rho_o h + b^2) W^2 v_i - \alpha b^t b_i \\ \tau = (\rho_o h + b^2) W^2 - (P + \frac{1}{2} b^2) - (\alpha b^t)^2 - D \\ B^k \end{bmatrix}$$

We have the corresponding flux terms:

$$f(q) = \begin{bmatrix} D v^i \\ S_j v^i + P \delta^i_j - \frac{b_j B^i}{W} \\ \tau v^i + P v^i - \alpha \frac{b^t B^i}{W} \\ B^k v^i - v^k B^i \end{bmatrix} \tag{100}$$

$$\Sigma(q) = \begin{bmatrix} 0 \\ T^{\mu\nu} \left( g_{\nu j, \mu} - \Gamma^\lambda_{\mu\nu} g_{\lambda j} \right) \\ \alpha \left( T^{\mu t} \left( \ln \alpha \right)_{, \mu} - \Gamma^t_{\mu\nu} T^{\mu\nu} \right) \\ 0 \end{bmatrix} \tag{101}$$

This spacetime has a few interesting features even well outside of the event horizon. If one wishes to demonstrate the effects of a black hole say a blob of matter, (like tidal forces) just setup a system with zero initial velocity, and some small gaussian distribution of matter density and hydrostatic pressure centered outside of the event horizon. Then evolve the codes as usual. We can observe the tidal flow of this object into the black hole. If nothing else this would be entertaining and possibly a good visual demonstration for new students.

Again, I am walking you through the basic tests and thought processes for developing fluid code.

Another essential test is if we set $M = 0$, we had better recover the Minkowski spacetime evolution.

A further simulation performed with the hydrodynamic code comes from the work by Font etal wherein they simulate axisymmetric relativistic Bondi–Hoyle–Lyttleton accretion. Their claim is that after some transient behaviour, a black hole travelling through uniform density and pressure space at a uniform velocity. I model this and will write about my conclusions later... I need to implement extreme values for the adiabatic constant. As well as log coordinates since this problem need resolution near the horizon.

As mentioned this metric has a coordinate singularity at $R = 2M$ so a more appropriate set of coordinates will need to be selected for evolution up to and including the event horizon. Coding issues definitely arise as one tends near the event horizon, especially if one performs the given magnetic field averaging, where the use of ghost cells is required. For the sake of credibility the Eddington Finkelstein coordinates will need to be implemented.

The Eddington-Finkelstein line element is

$$ds^2 = -\left(1 - \frac{2M}{r}\right) dv^2 + 2dvdr + r^2 d\theta + r^2 \sin^2\theta d\phi$$

The basics behind Bondi–Hoyle–Lyttleton accretion is that we have a black hole travelling through a fluid of uniform density and pressure at a constant velocity. The boundary condition setup is quite logical, at the upstream location we have inflow, saying that the background density is uniform in all space. At the rear, we have outflow, where the matter once it falls out of the domain of interest may disappear, having no expected effect on the domain of interest. This is for the outside boundaries for the domain. On the boundary where the black hole exists we expect outflow in all directions. Outflow is a general term in this case, as what it means in this case is that the fluid will enter the black hole's event horizon, and will not come back. To smooth the outflow one uses extraploated outflow for vector quanitities and cell copying for scalar quantities as described in Font et al. This author found that the linear extrapolation was not necessary if on uses enough resolution (large enough number of cells) in the evolution. This result agrees with Font et al.

My simulations using this background may be found:

http://laplace.physics.ubc.ca/People/ajpenner/movies/movies.html

These have $M = 1, a = 0$

longer movies will exist when I finish parallelizing the code.

### 20.3.4 Kerr Spacetime Background

For the Kerr spacetime in Boyer-Linquist coordinates we have the line element:

$$ds^2 = -\left(1 - \frac{2Mr}{\Sigma}\right) dt^2 - \frac{4aMr\sin(\theta)^2}{\Sigma} dtd\phi + \frac{\Sigma}{\Delta} dr^2 + \Sigma d\theta^2 + \left(r^2 + a^2 + \frac{2a^2 Mr\sin(\theta)^2}{\Sigma}\right) \sin(\theta)^2 d\phi^2 \quad (102)$$

Where we use

$$\Sigma = r^2 + a^2\cos(\theta)^2$$

$$\Delta = r^2 - 2Mr + a^2$$

$M$ is the mass of the rotating object $a = \frac{J}{M}$ is the rotation of the black hole, with angular momentum $J$ as before we use Geometric units.

This metric requires all elements of the 3+1 decomposition, so I will not restate the fluid equations.

As with the Schwarzschild metric we have singularities at the event horizon that can be circumvented by use of the Kerr-Schild coordinates. This metric leaves us with a line element

$$ds^2 = -\left(1 - \frac{2M}{r_s}\right) dt^2 + \frac{4M}{r_s^2} dtdr_s + \left(1 + \frac{2M}{r_s}\right) dr_s^2 + r_s^2 d\theta + r_s^2 \sin^2\theta d\phi$$

with

$$r_s = r\left(1 + \frac{M}{2r}\right)$$

clearly the singularity at the origin still exists, but since that is hidden by the event horizon, it is of little concern.

More interesting features from Bondi-Hoyle accretion occur here, now that the black hole is rotating. We see a twist in the inflowing matter. Originally this was investigated by Font and Ibanez both with the Boyler-Lindquist coorindates and with the Kerr–Schild coordinates.

Their claim is that the accretion disk becomes stable after some transient time. However their analysis was sparse when considering the parameter space available. Further they did not include contributions from magnetic fields.

My simulations using this background may be found:

http://laplace.physics.ubc.ca/People/ajpenner/movies/movies.html

These have $M = 1, a = 0.5$

longer movies will exist when I finish parallelizing the code.

# 21 Vorticity and Helicity

The vorticity of a fluid is argued to be a fundamental property of the fluid, moreso than the velocity itself. Naturally one needs to define this quantitiy in full spacetime: The 4-vorticity of a hydrodynamic system is defined to be

$$\omega^{\alpha} = \epsilon^{\alpha\beta\gamma\delta} u_{\beta} u_{\delta;\gamma}$$

For the magnetic field case, the vorticity analogue is the magnetic field itself.

$$B^{\alpha} = \epsilon^{\alpha\beta\gamma\delta} u_{\beta} A_{\delta;\gamma}$$

With these (typically proven the other way around) we have the vorticity pseudotensors.

$$\omega^{\alpha\beta} = (hu_{\beta})_{,\alpha} - (hu_{\alpha})_{,\beta}$$

and

$$F^{\alpha\beta} = (A_{\beta})_{,\alpha} - (A_{\alpha})_{,\beta}$$

From Bekenstein we know of three helicity relations that are expected to be globally conserved:

The fluid helicity

$$H_f^{\alpha} = {}^{*}\omega^{\alpha\beta}(hu_{\beta})$$

The magnetic helicity

$$H_m^{\alpha} = {}^{*}F^{\alpha\beta} A_{\beta}$$

The magnetic fluid helicity (cross helicity)

$$H_{fm}^{\alpha} = {}^{*}F^{\alpha\beta}(hu_{\beta}) = hB^{\alpha}$$

where $h$ is the relativistic enthalpy as defined in an earlier section. He follows each of these with a proof of their conservation which is trivially true in the case of isentropic evolution, fortunately my system is treated as isentropic.

# 22 Turbulence

There are several outstanding questions about turbulence in fluids. Not the least being, how does one go about measuring turbulence? Some groups working on Newtonian fluid dynamics have come up with some statistical methods of measuring turbulent velocities as the variance of the individual field components.

$$v_i^{turb} = \sqrt{\bar{v_i^2} - \bar{v_i}^2}$$

Since the 4-velocity is more natural to relativistic systems, this procedure would need to be generalized and possibly used as a measure of relativistic turbulence.

Here are a short list of a few of the papers I used to get my research moving. All of these (minus the textbooks) are available on my webpage http://laplace.physics.ubc.ca/Members/ajpenner/MHD.html

# References


[1] Randall LeVeque, *Finite volume methods for hyperbolic problems*, Cambridge, 2000

[2] M.M. May and R.H. White, *Hydrodynamic calculations of general relativistic collapse*, Phys. Rev. D, 141, 1232-1241, 1966

[3] L. Antón et al., *Numerical 3+1 general relativistic magnetohydrodynamics: A local characteristic Approach*, arxiv 0506063, June, 2005

[4] Sergey V Golovin, *Singular vortex in magnetohydrodynamics*, J. Phys. A: Math. Gen. 38 4501-4516.

[5] Scott Noble, *A numerical study of relativistic fluid collapse*, PhD Thesis, December 2003, University of Texas.

[6] Evans, Hawley, *Constraint Preserving Transport for Magnetohydrodynamics*, Frontiers in Numerical Relativity, 179, 1989.

[7] Hawley, DeVillars, *Numerical Method for General Relativistic Magnetohydrodynamics*, submitted Astrophysics Journal.

[8] Ignacio Olabarrieta, *Relativistic Hydrodynamics and other topics in Numerical Relativity*, PhD Thesis, UBC.

[9] Noble, Gammie, McKinney, *Primitive Variable Solvers for Conservative General Relativistic Magnetohydrodynamics*, submitted Astrophysics Journal.

[10] John F. Hawley, Steven A. Balbus, & James M. Stone, *A Magnetohydrodynamic Nonradiative Accretion Flow in Three Dimensions*, Astrophysical Journal Letters, 554, (2001)

[11] Jacob D. Bekenstein, *Helicity Conservation Laws for Fluids and Plasmas*, Astrophysical Journal, 319, 207-214 (1987)